# Implementation of Optical Response of Thin Film Transistor with Verilog-A for Mobile LCD Applications

Keiichiro Ishihara*
Sony Corporation, Japan
Keiichiro.Ishihara@jp.sony.com

Yasuhiko Iguchi
Sony Corporation, Japan
Yasuhiko.Iguchi@jp.sony.com

Makoto Watanabe
Sony Corporation, Japan
MakotoD.Watanabe@jp.sony.com

Takeyuki Tsuruma
Sony Corporation, Japan
Takeyuki.Tsuruma@jp.sony.com

Takeshi Sawada
Sony Corporation, Japan
Takeshi.Sawada@jp.sony.com

Yasuhito Maki
Sony Corporation, Japan
Yasuhito.Maki@jp.sony.com

## ABSTRACT

In this paper, a contribution of Verilog-A to the optimum design of liquid crystal displays (LCDs) is presented. The Verilog-A module for estimating the photo-leakage current was attached to a built-in thin film transistor (TFT) model as an independent instance. Sufficient accuracy, desired speed, and good computational stability have been obtained for LCD design. This plug-in approach can facilitate to implement some additional effects to a built-in model already provided in commercial circuit simulators.

## 1. INTRODUCTION

Ever increasing advances in product quality are demanded of the LCD industry. These requests come hand in hand with expectations for enhanced performance, such as high brightness, high contrast, fast response, low power consumption, compact shape, etc. Optimum levels in both optical and electrical aspects must be reached in order to design LCDs which can endure such a fierce market. An LCD design incorporating optical properties have been in demand for the purpose.

Conventional transistors are fabricated on crystalline wafers of silicon cut from a crystal boule grown from a melt. On the other hand, TFTs are fabricated on silicon generally deposited on glass substrate. One of the most practical uses of TFTs is as a switching-device in an LCD's drive circuit and pixel area. In the drive circuit, TFTs can be shielded from light in various forms. TFTs in the pixel area, however, are exposed to light, and are therefore liable to be under influence. Fig. 1 is a cross sectional view of a typical pixel. The pixel is composed of TFT, storage electrode, pixel electrode, common electrode, and liquid crystal. Transparent electrodes are employed for common and pixel electrodes for display uses. Opaque factors should be kept minimum to achieve high brightness. Both backlight and ambient light enter from the bottom and top of the cell, consequently changing the characteristics of pixel transistors. Pixel transistors are required to maintain pixel voltage for significant periods of time. Inaccurate estimation of the variance caused by light exposure could therefore, in effect, lay the grounds for malfunctioning in the display property, i.e., flicker, vertical cross-talk, and un-uniformity. As the performance of the display property depends largely on the capability of the pixel transistors, determining its characteristics in the designing process is vital.

The development of transistor models which increase speed and accuracy of SPICE simulation is a goal pursued by many research institutes and universities. Currently, commercial SPICE simulators are innately equipped with many of these models, giving users the liberty to decide on the one to meet their needs. Many such models show accuracy with regard to expressing adequate device characteristics. None of the TFT models, however, has taken into consideration the influence of light.

As the majority of models currently provided by EDA vendors are not open to modification, model developers face the need to create original transistor models in order to take into account the effect of light. As new models need to be equipped with levels of speed and accuracy compatible to those already on the market, synthesis of such models demands much effort of developers, and multiple evaluations must be performed to ensure its validity.

If external factors on semiconductor devices are independent of characteristics calculated by proven models, these factors can be added to the characteristics calculated by the models. This way, developers only need to model phenomena which are not given or expressed in the model. By overcoming the limitation, with some assumptions this method can be utilized in the case of optical illumination.

In this paper, we present an efficient and accurate method

*Mobile Display Business Group, Sony Corporation, 4-14-1 Asahi-cho, Atsugi-shi, Kanagawa, 243-0014, Japan

for predicting circuit behavior considering optical response of semiconductor devices. Using Verilog-A language, we developed a photo-current module and connected it to a proven device model to perform accurate and fast simulations.

In section 2, a method and model to include the effect of optical illumination in the SPICE simulation with improved convergence is introduced. The code in Verilog-A is shown in section 3. The model validity and its performance are discussed in section 4. The applications of this model to LCD design is illustrated in section 5. The paper is concluded in section 6.

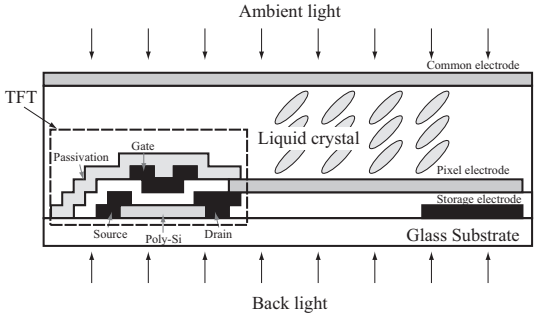


Figure 1: Cross sectional view of a pixel in a typical LCD.

# 2. MODEL

## 2.1 Model overview

Fig. 2 is a schematic of a photo-current module connected to a TFT device model. The photo-current module is a two terminal instance written in Verilog-A and is connected to the source and the drain node of the TFT. This module calculates photo-leakage current ($I_{photo}$) according to the applied voltage and given light intensity. Here, the photo-current module is modeled as a current source whose input is voltage, light intensity, and width of the transistor to which it is connected.

One of the most popular poly-silicon TFT device models available in many simulators is the Rensselaer Polytechnic Institute (RPI) model[2]. It accurately expresses DC and AC characteristics of poly-silicon TFT in supposed operating conditions. The RPI model was chosen as the transistor model to connect the photo-current module. Because transistor and photo-current module are connected in parallel, the output current from the transistor model ($I_d$) and the photo-current module ($I_{photo}$) are simply added to express the effect of photo-generation.

## 2.2 Photo-current module

There are two generation paths related to the photo-leakage current.

1. Photo-carriers generated inside the depletion region.

   When the carriers are generated in the depletion region, they are separated by the electric field in this region, thus, an increase in leakage current is observed.

2. Photo-carriers generated outside the depletion region.

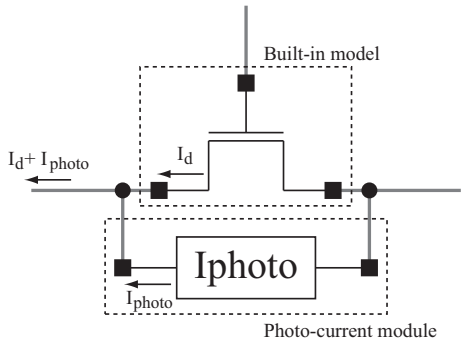


Figure 2: Schematic of TFT with photo-current module.

   Some carriers generated at just outside of depletion region are diffused into the depletion region by the concentration difference. They are accelerated by the electric field in the depletion region, then an increase in leakage current is observed.

The former can be defined as a drift component of photo-leakage current, and the latter, a diffusion component. It is preferable to consider both components in the module. However, diffusion current is already given in the leakage current of the RPI model. We neglected the diffusion component of the photo-leakage current because we empirically knew that the drift component of photo-leakage current is dominant compared to the diffusion component. By doing so, $I_{photo}$ can be modeled as an independent block of current source. Consequently, SPICE simulation considering photo-leakage current becomes much simpler.

The photo-generation rate $G$ is given by the following equation[1]:

$$G(x) = \int_{\lambda_{min}}^{\lambda_{max}} \alpha(\lambda, x)\Phi(\lambda, x)e^{-\int_0^x \alpha(\lambda,x)dx} d\lambda \qquad (1)$$

Here, $\Phi(\lambda)$ is photon flux, $\alpha$ is absorption coefficient, $\lambda$ is wavelength and $x$ is distance from the incident surface. By assuming that absorption coefficient does not vary with wavelength and position, and that $\Phi$ is the total photon flux of all wavelengths, Eq. (1) is simplified to

$$G(x) = \alpha\Phi(x)e^{-\alpha x} \qquad (2)$$

Photon flux at incident surface $\Phi(0)$ is given by

$$\Phi(0) = \frac{P_{in}}{h\nu}(1 - R) \qquad (3)$$

where $P_{in}$ is intensity of incident light, h is plank's constant, $\nu$ is frequency, and $R$ is reflection coefficient. Assuming that the silicon layer in TFT is so thin that incident light does not decay in the silicon and that there is no reflection at the surface, Eq. (2) and (3) are simplified to

$$G = \frac{P_{in}\alpha}{h\nu} \qquad (4)$$

All the carriers generated in the depletion region are drifted by the field in the depletion region without recombination;

i.e., carriers generated in the depletion region are given by the product of generation rate and the volume of the depletion region. Photo-leakage current $I_{photo}$ generated in the depletion region is given by

$$I_{photo} = qt_{S_i}wl_{dep}G \tag{5}$$

where $q$ is elementary charge, $t_{S_i}$ is thickness of silicon layer, $w$ is device width and $l_{dep}$ is depletion length.

By solving Poisson's equation at p-n junction, depletion length is given by Eq. (6).

$$l_{dep} = \sqrt{\frac{2\epsilon_{Si}(N_a + N_d)\phi_{bi}}{qN_aN_d}} \tag{6}$$

Where $\epsilon_{Si}$ is permittivity of the silicon, $N_a$ is acceptor concentration, $N_d$ is donor concentration and $\phi_{bi}$ is built-in potential. When the voltage is applied across drain and source, $\phi_{bi}$ in Eq. (6) is replaced by $\phi_{bi} + V_{ds}$, where $V_{ds}$ is the extrinsic drain-source voltage.

By combining Eq. (4), (5), and (6), current calculated in photo-current module is given.

## 2.3 Convergence issue

When no external voltage is applied to a device, SPICE simulators assume no current is flowing in the device because they are based on ohm's law. This assumption is only true when the device is not exposed to the light. When optical illumination exists, photo-leakage current flows even if voltage is not applied. This may cause convergence difficulties in SPICE simulations. To avoid this, it is desirable that photo-leakage current be zero when no voltage is applied. To do so, $I_{photo}$ in Eq. (5) is modified to

$$I_{photo_{mod}} = I_{photo} \cdot tanh^2(\alpha_{mod} \cdot V_{ds}) \tag{7}$$

where $\alpha_{mod}$ is a positive number. The shape of the function $tanh^2(\alpha_{mod} \cdot V_{ds})$ is shown in Fig. 3. It is a continuous function whose value rapidly drops to 0 around $V_{ds} = 0$. As shown in the figure, $\alpha_{mod}$ is used to change the slope of the drop. It is required that $\alpha_{mod}$ be large enough for $tanh^2(\alpha_{mod} \cdot V_{ds})$ to be close to 0 around $V_{ds} = 0$, and at the same time, optimized to achieve the convergence requirement of SPICE simulations.

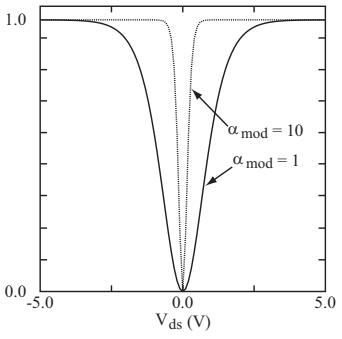


Figure 3: The shape of the function $tanh^2(\alpha_{mod} \cdot V_{ds})$

# 3. CODING IN VERILOG-A

For its flexibility and capability of simple implementations to circuit simulators, we chose Verilog-A language for describing our module. Listing 1 is the excerption of Verilog-A code used in photo-current module.

In lines 3-5, the module for a photo-leakage current with two interface ports d and s is defined.

In lines 18-22, the effective device width $w_{eff}$ is calculated. Here, $w_{eff}$ is calculated in a similar way to the RPI model, which is determined by a given $acm$ value. The cases for $acm = 0$ and 1 are shown in this excerption. The corresponding model parameters should be selected.

In lines 25-26, depletion length $l_{dep}$ is calculated for given applied voltage and model parameters.

In lines 28-29, photo-leakage current $I_{photo}$ is calculated according to calculated $w_{eff}$, $l_{dep}$, given light intensity $brightness$, and model parameters.

In lines 31-32, modification for improving convergency of the SPICE simulation is applied.

In lines 34-37, photo-leakage current is supplied to the external circuit.

Listing 1: Photo-current model in Verilog-A

```
1  // Verilog−A for Photo−leakage current module
2
3  module iphoto(d, s);
4  inout d, s;
5  electrical d, s;
6  ...
7  analog begin
8  begin
9   if (V(d, s) >= 0.0) begin
10    mode = 1;
11    vds = V(d, s);
12   end
13   else begin
14    mode = −1;
15    vds = −V(d, s);
16   end
17
18   if (acm == 0)
19    weff = w * scale;
20   else if (acm == 1)
21    weff = (w * scale * wmlt + xw − 2 * wd
22 * scale);
23
24 ...
25   ldep = sqrt(2.0 * 'EPSILON_SI * (eb + vds)
26 / ('Q_E * na * nd) * (na + nd));
27 ...
28    iphoto = 'Q_E * tsi * weff * ldep *
29 (brightness * alpha) / ('H * 'C / lambda);
30
31    iphoto = iphoto * pow(tanh(alphamod
32 * vds), 2);
33
34   if (mode > 0)
35    I(d, s) <+ iphoto;
36   else
37    I(d, s) <+ −iphoto;
38
39 end
40 end
41 endmodule
```

# 4. MODEL EVALUATION

## 4.1 Validity

Results of comparison between the measurement and simulation of the $I_d - V_g$ characteristics of poly-silicon TFTs with various light intensities are shown in Fig. 4 (a) TFT 1 and (b) TFT 2. TFT 1 and 2 have the same layer thickness and structure but are different in device width and length. Here, DC simulation in dark condition and two different light intensities are performed. The input intensity *brightness* of the light "intensity 1" in Fig. 4 is weaker than that of "intensity 2", and this is in accordance with the results. Simulation results of dark conditions are similar to the results calculated using only the RPI model. The above threshold current characteristics are also mainly calculated using the RPI model since the effect of optical illumination is overshadowed by the on-current. Off-current of "intensity 1" and "2" are mainly calculated by the photo-current module. A good agreement is observed with the experimental results in both illumination conditions for TFT 1 and 2. The fitting error of off-current of measured and simulated results are shown in Table. 1. The errors for all cases show a high degree of precision, which prove the competency of this model.

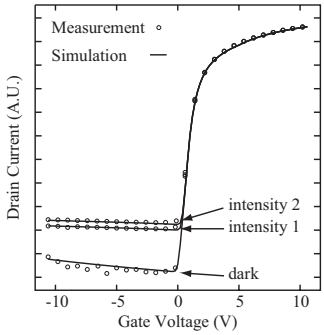


(a) TFT 1

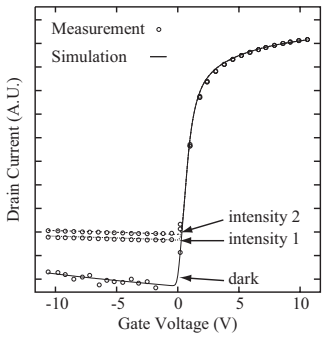


(b) TFT 2

Figure 4: Measured (dotted) and simulated (solid-line) $I_d - V_g$ characteristics of TFTs. (a) TFT 1 and (b) TFT 2 are the same TFT with different device width and length.

Table 1: The fitting error of measured and simulated leakage current of TFT 1 and 2 at intensity 1 and 2.

| Intensity | TFT 1 | TFT 2 | Avg. Error |
|---|---|---|---|
| Intensity 1 | 1.23 % | 5.68 % | 5.33 % |
| Intensity 2 | 9.43 % | 3.11 % | 4.40 % |

## 4.2 Performance

One important issue regarding circuit simulation in designing LCDs is accuracy. But even if it is accurate, designers do not want to use the simulation if it does not finish in the desired period of time. Fig. 5 is the comparison between the runtime of simulations performed without photo-current module (only the RPI model) and with photo-current module. Because simulation with photo-current module involves more equations, runtime is increased, but the difference is only 1.06 times longer. One can conclude that the effect of 1.06 times amplification in simulation runtime on the efficiency of the circuit design can be ignored.

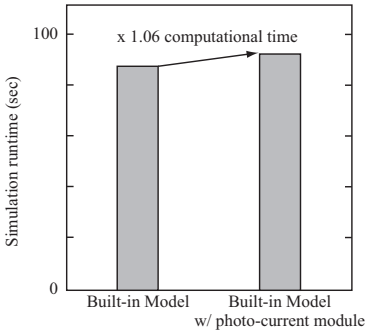


Figure 5: Simulation runtime comparison between built-in model and built-in model with photo-current module.

# 5. APPLICATION

In this section, two examples of applying photo-current module to TFT-LCD design are presented. Fig. 6 is a schematic diagram of active-matrix TFT-LCD panel (left) and electric circuit diagram of a pixel (right). Each pixel is composed of TFT, storage capacitor ($C_{sc}$), and liquid crystal ($C_{LC}$). From an electrical circuit point of view, liquid crystal behaves as a capacitor whose capacitance varies with applied voltage and time. On the other hand, storage capacitor is a static capacitance whose one function is to hold voltage for one frame time.

The principle of operation is described as follows[4]. Here, pixels are addressed one line at a time. When a gate line is addressed by V driver, a positive voltage pulse is applied to the line turning on all the transistors along the row. The transistors behave as switches transferring electrical charges to the LC capacitors from the respective columns. When addressing other rows, a negative voltage is applied to the gate lines turning off all the transistors along the line and holding the electrical charges in the LC capacitors for one frame time until the line is addressed again. The DC voltage $V_{com}$ is applied to the storage line and one terminal of $C_{LC}$. To avoid the ionic material concentration on a surface, it is desirable that the driving voltage across the liquid crystal cell be alternating in time. This is achieved by switching the polarity of the signal line in an alternative frame.

During the hold period, the voltage across the liquid crystal does not remain constant. One cause of this phenomena is the leakage from the transistor. The leakage current of the TFTs should be low so that the charge stored in $C_{sc}$ and $C_{LC}$ will not leak out and affect the display property. As

can be easily suspected, an increase in conductivity by optical illumination may degrade the appearance of the panel. Therefore, it is important to know the requirement for the leakage current of the TFTs.

Fig. 7 is a schematic of the circuit used in the examples. A TFT is connected with the photo-current module, and a storage capacitor and liquid crystal are connected as well. Characteristics of the liquid crystal were modeled in Verilog-A language in our previous work[3], and this model is employed in this case for more realistic LCD simulations. Voltage sources $V_g$, $V_{sig}$ and $V_{com}$ are applied accordingly. Here $V_{pix}$ is defined as the node between liquid crystal module and drain of the TFT.

Fig. 8 (a) is one simulated example of Fig. 7. A transient analysis is performed and $V_{pix}$ is calculated with given voltage sources; $V_g$, $V_{sig}$, and $V_{com}$. For simplicity, a DC voltage is applied to $V_{com}$. As a positive voltage is applied to $V_g$, $V_{pix}$ reaches the voltage given by $V_{sig}$. A negative voltage is then applied to $V_g$ to turn off the transistor, and $V_g$ remains negative until the next frame time. At the moment when $V_g$ turns from positive to negative, $V_{pix}$ is slightly changed by the coupling. As shown in the figure, $V_{pix}$ cannot retain the same voltage. This is because the charge stored in $C_{sc}$ and $C_{LC}$ leak away by the leakage of the transistor. This phenomenon become crucial when the amount of leakage is large, like in the case of optical illumination. Since the liquid crystal cell sees the voltage difference between $V_{pix}$ and $V_{com}$, change in $V_{pix}$ results in unintentional driving voltage of the liquid crystal cell. In the next frame time, polarity of $V_{sig}$ is changed, and similar characteristics are observed in $V_{pix}$. Fig. 8 (b) shows comparison of change in $V_{pix}$ in different light intensities. In the dark case, $V_{pix}$ remains almost constant. When optical illumination exists, the leakage of transistor becomes significant, thus, change in $V_{pix}$ is observed in a frame time. For both cases, the difference in $V_{pix}$ caused by photo-leakage current are about a few tenths of volts. For typical LCDs in the market today, the voltage difference among each gray level is several tens of millivolts. To reduce its effect on display property, the following optimizations should be applied during LCD design processes.

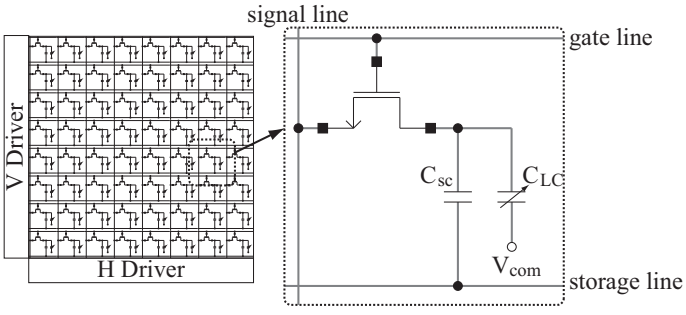


Figure 6: Schematic diagram of LCD panel (left) and electric circuit diagram of a pixel (right).

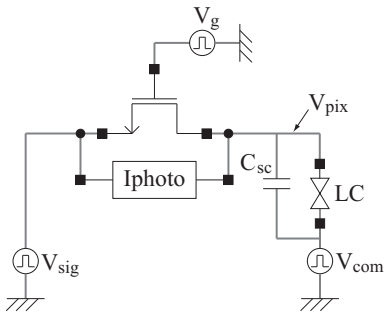


Figure 7: Typical pixel circuit of LCD.

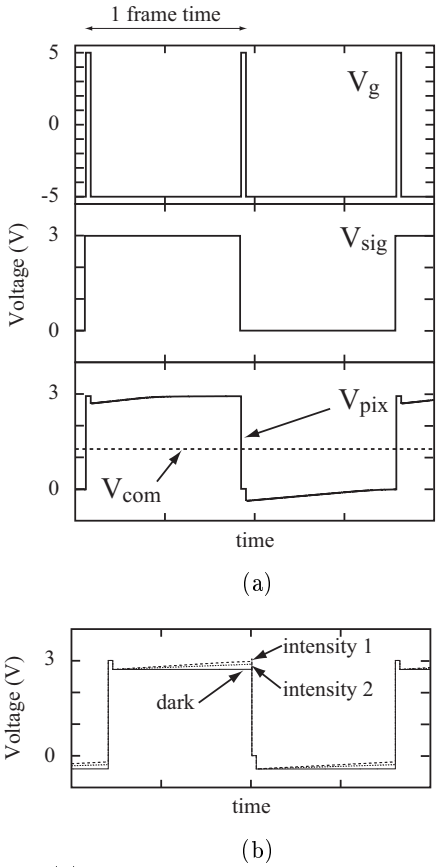


Figure 8: (a) Example of each voltage for two frame time. (b) Comparison of $V_{pix}$ in different light intensities.

## 5.1 $V_{com}$ optimization

Liquid crystal is driven by the voltage $V_{pix} - V_{com}$. As shown in Fig. 8, liquid crystal sees a positive and negative voltage in each consecutive frame time. Difference between the driving voltages of the liquid crystal cells in each frame time lead to the difference in the transmittance in alternate frames, which is known as the problem of flicker. Flicker can be minimized by applying the optimal $V_{com}$ voltage, which realize the minimum change in $V_{pix} - V_{com}$. Fig. 9 is the transient transmittance vibration dependencies on light intensities. Here, AC voltage is applied to $V_{com}$, as in most contemporary LCDs. Each simulation is performed with optimal conditions, i.e., optimum $V_{com}$ is used for each case.

As light intensity increases, the transmittance in alternate frames gradually varies even if optimal condition is used. It shows how narrow the window of LCD design is on $V_{com}$.

As stated, photo-leakage current changes $V_{pix}$, and makes driving voltage uneven in consecutive frame times. Fig. 10 shows simulated flicker levels with various $V_{com}$ voltages. The flicker level is calculated by taking Fast Fourier Transformation of transmittance in both positive and negative frame times. It is said that flicker will not appear in human eyes for flicker levels below $-20 \sim -30$ dB. For dark condition, flicker levels drop to a minimum value of $-40$ dB at $V_{com} = -0.4$ V. Here, the optimal $V_{com}$ for dark condition can be said to be $-0.4$ V.

As the amount of photo-leakage current increases, the minimum value for the flicker level rises and a slight change in optimal $V_{com}$ is observed. Since only one $V_{com}$ value can be chosen in an LCD, the $V_{com}$ value to meet the requirement for all conditions must be chosen in the design process. For this case, $V_{com}$ should be set to about $-0.35$ V.

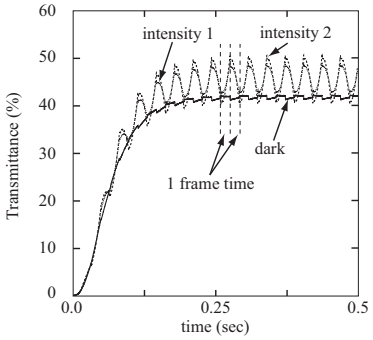


Figure 9: Flicker phenomenon in LCDs with different light intensities.

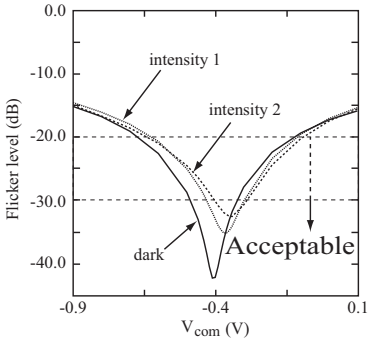


Figure 10: Flicker level dependency on $V_{com}$.

## 5.2 $C_{sc}$ optimization

As stated, photo-leakage current causes changes in flicker levels. One solution to minimize the effect of photo-leakage current on flicker level is to increase the storage capacitance $C_{sc}$. Fig. 11 is the dependency of flicker level on the storage capacitance. As storage capacitance increases the flicker level decreases regardless of the light intensity. This is simply because more capacitance results in better holding of the charge. Since storage capacitor is placed in the pixel area as shown in Fig. 1, and generally its capacitance is controlled by the size, increasing the capacitance leads to less aperture ratio, thus light throughput decreases. LCDs with desired aperture ratio for the minimum flicker level can be designed by this simulation.

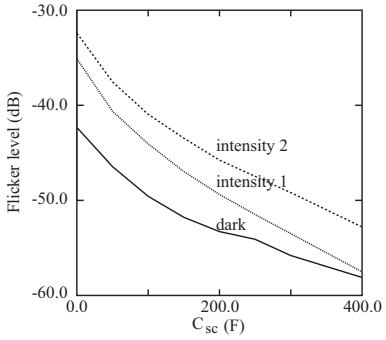


Figure 11: Flicker level dependency on $C_{sc}$.

# 6. CONCLUSION

By employing Verilog-A language, accurate and expeditious circuit simulation considering the effect of optical illumination on transistors has been achieved using the above proposed method. The validity of the model was verified by checking the agreement with measured data, and the average accuracy level of below 6% was obtained for leakage current. At the same time, the simulation runtime with photo-current module of only 1.06 times more than the one without photo-current module was attained. This method has enabled the detection of possible causes of malfunctioning in the LCD property as early as during the designing process. At the same time, it provides useful information for the optimum LCD design. Implementation of this method will allow us to contemplate the optical responses in not only TFTs but in other semiconductor devices such as diodes as well.

# 7. ACKNOWLEDGMENT

The authors would like to thank Dr. M. Ikeda and Y. Kuwahara for valuable suggestions on this work and Sony Mobile Display Corporation for providing samples.

# 8. REFERENCES

[1] C. Amano, H. Sugiura, M. Yamaguchi, and K. Hane. Fabrication and numerical analysis of algaas/gaas tandem solar cells with tunnel interconnections. IEEE Trans. Electron Devices, 36:1026–1035, 1989.

[2] B. Iniguez, Z. Xu, T. A. Fjeldly, and M. S. Shur. Unified model for short-channel poly-si tfts. Solid-State Electronics, 43:1821–1831, 1999.

[3] M. Watanabe, K. Ishihara, T. Tsuruma, Y. Iguchi, Y. Nakajima, and Y. Maki. Macro-modeling of liquid crystal cell with veriloga. Proceedings of the 2007 IEEE International Behavioral Modeling and Simulation Workshop, pages 132–137, 2007.

[4] P. Yeh and C. Gu. Optics of Liquid Crystal Displays. John Wiley and Sons, Inc., 1999.